Journal of Marine Research, 53, 201–210, 1995

Local and remote forcing of the barotropic transport through a periodic gap in a basin with bottom topography

by Alexander Krupitsky[1]

ABSTRACT

The effect of bottom topography H on the barotropic transport through a periodic gap in a basin with large-scale bottom topography is studied. The results obtained generalize previous findings for the case of a zonal channel (Wang and Huang, 1995; Krupitsky and Cane, 1994). An asymptotic approximation is found for the zonal transport on a β-plane when all f/H isolines are blocked by the solid boundaries. It is shown that to leading order, the transport through the gap (i) is independent of friction similar to a western boundary current; (ii) is inversely proportional to R, the range of values of f/H that exist on both parts of the solid boundary. The transport depends on the latitude of the equatorward side of the gap, but not on the poleward one. The transport is forced by a mean wind in the area poleward of the equatorward side of the gap and in two remote forcing regions discussed in the text.

1. Introduction

Simple barotropic models of the Antarctic Circumpolar Current (ACC) have attracted researchers for more than forty years. Their appeal continues for at least two reasons. First, since the Southern Ocean is weakly stratified one expects that the barotropic model would be a zero order approximation to reality. Second, most numerical models integrate the vertically averaged equations separately from the rest. Thus a simple barotropic model may give significant insight into the results of complicated general circulation models.

The key question of circumpolar dynamics is what balances the input of momentum and vorticity by wind. In the early models of the ACC developed by Kamenkovich (1960, 1962) and extended by Johnson and Hill (1975) the wind input was balanced by the bottom friction. In these models it was assumed that the contours of potential vorticity f/H (f being the Coriolis parameter and H the depth) close around Antarctica. Such a configuration effectively stipulates the breakdown of the Sverdrup balance in the circumpolar domain. Since the pressure gradient cannot build up on the closed contour, the friction, no matter how small the coefficient is, must balance the wind input. This is the essence of a problem encountered by many flat-bottomed

1. Lamont-Doherty Earth Observatory of Columbia University, Palisades, New York, 10964, U.S.A.

models (e.g. Hidaka and Tsuchiya, 1953; Bryan and Cox, 1972): either the friction coefficient or the ACC transport was unreasonably high (Hidaka dilemma).

Munk and Palmen (1951) were the first to suggest that it is topographic pressure torque that balances the input of vorticity by the wind stress curl. There are significant submarine ridges which allow transfer of horizontal momentum to the solid earth. Eddy resolving experiments by McWilliams *et al.* (1978), Wolff and Olbers (1989), Wolff *et al.* (1990), and Wolff *et al.* (1991) have shown that the topographic pressure drag is the major term in momentum balance.

Krupitsky and Cane (1994) (hereafter KC) considered almost inviscid wind driven flow in a zonal channel with the large-scale piecewise linear topographic relief sufficiently high that all f/H contours are blocked by the sidewalls. They found that the zonal channel transport is independent of friction, similar to the Sverdrup transport in a basin. Certain parts of the sidewalls act as "quasi-western" boundary layers where the circulation closes. Similar results were obtained by Wang and Huang (1995) who studied the case of a ridge in an otherwise flat channel.

A key assumption in these models is that the sidewalls are vertical. If the depth were allowed to gradually vanish at the sidewalls, then inevitably there would be a band of closed f/H contours around Antarctica and the dynamics suggested by Kamenkovich (1960, 1962) would apply. There are several reasons to choose the vertical sidewalls over the gradually sloping bottom: (i) the width of the shelf is small compared to the width of the ACC which varies between 800 and 1500 km; (ii) even a small horizontal viscosity (neglected in the analytical models mentioned above) is likely to shut down the shelf-trapped circumpolar current allowed by the existence of f/H contours closed near boundaries; (iii) shallow coastal currents along the closed f/H contours are not observed in reality.

Since the path of the real ACC is remote from solid boundaries except in the Drake Passage, removing the zonal walls which artificially separate the circumpolar region from the rest of the World Ocean is a useful extension of the previous work, a step toward improving the verisimilitude of the simplified analytical models. We still assume a highly idealized geometry: a rectangular basin with a large-scale topography and a periodic gap of zero length imitating the Drake Passage. The essential assumption here is that the sides of the gap are not connected by f/H contours. This means that zonal scale of topographic variations is assumed large compared to the length of the Drake Passage. Wang (1994) considered a geometry in which the only topographic feature was a narrow ridge fully contained within the Drake Passage, and high enough to block all f/H contours. Our results coincide in finding an inviscid limit of the transport through the gap but differ significantly in dependence of the transport on model parameters.

2. The model

The geometry of the model is sketched in Figure 1. The model domain is a rectangular basin $0 \leq x \leq 1, y_n \leq y \leq y_s$ with a periodic gap $0 \leq y \leq d$ on the

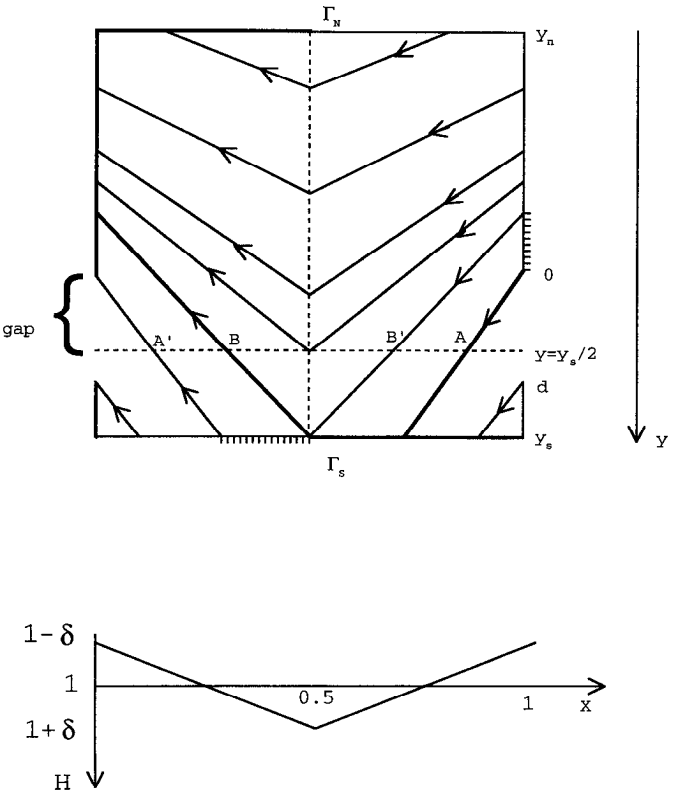

Figure 1. A schematic of the characteristics f/H, bottom topography and and boundary layers. Points A, A′, B and B′ are discussed in the text.

meridional sides. We assume that the longitudes of the gap and the depth minimum coincide. We could treat a more complicated geometry with three separate oceans to the north of the circumpolar region but since the mathematical treatment would be essentially the same, we consider the simpler case of a single ocean. The part of the solid boundary to the north of the gap is designated Γ_N, the part to the south of the gap Γ_S.

The equations of the present model are identical to those of KC. A barotropic flow on a β-plane driven by a zonal wind τ is governed by the nondimensional potential vorticity conservation equation

$$\nabla \cdot \left(\frac{\epsilon}{H^2} \nabla \psi \right) + J\left(\psi, \frac{f}{H} \right) = -\frac{1}{H} \frac{\partial \tau}{\partial y}, \tag{1}$$

where J is the Jacobian and

ψ is the transport stream function: $\nabla\psi = (vH, -uH)$;

u, v are the vertically averaged zonal and meridional velocities, respectively; the x, y and z axes are directed eastward, southward and downward, respectively, with $y = 0$ at the latitude of the northern (equatorward) side of the gap;

$H = 1 + \delta h$ is the depth, $h = h(x)$ is $O(1)$ nondimensional topography, $-1 \leq h \leq 1$; $\delta \leq O(10^{-1})$;

$f = 1 + \beta(y - y_s/2)$ is the Coriolis parameter increasing to the south;[2]

ϵ is the bottom friction coefficient.

The boundary conditions are

$$\psi|_{gap,x=0} = \psi|_{gap,x=1}, \tag{2}$$

$$\psi|_{\Gamma_N} = 0, \tag{3}$$

$$\psi|_{\Gamma_S} = -T. \tag{4}$$

The problem is to find T, the unknown transport through the gap.

As in KC, the wind stress τ is taken to be purely zonal and depends only on latitude. As discussed in KC, if the topography is small enough then there are closed f/H isolines encircling Antarctica and a rather large transport results. There is a minimum topographic height δ_{cr} such that f/H lines no longer close: if $\delta = \delta_{cr}$ one f/H isoline connects the southern tip of Γ_N (the analog of Cape Horn in our model) with the point of maximum depth of Γ_S. This occurs for the value δ_{cr} such that

$$\frac{f(y = 0)}{1 - \delta_{cr}} = \frac{f(y = y_s)}{1 + \delta_{cr}}$$

or

$$\delta_{cr} = \frac{f(y = y_s) - f(y = 0)}{f(y = y_s) + f(y = 0)} = \frac{y_s\beta}{2}. \tag{5}$$

If $\delta > \delta_{cr}$ there is a range R of f/H lines that intersect both boundaries:

$$R = \max (f/H)_{\Gamma_N} - \min (f/H)_{\Gamma_S}$$

$$= \frac{1 - y_s\beta/2}{1 - \delta} - \frac{1 + y_s\beta/2}{1 + \delta} = \frac{2}{1 - \delta^2}(\delta - \delta_{cr}) \approx 2(\delta - \delta cr).$$

KC have shown that if $\delta > \delta_{cr}$ then there is an inviscid limit to the transport in the channel with vertical walls. Here we extend this result to the more realistic geometry

2. Our unconventional right-handed coordinate system is convenient for the Southern hemisphere because H, f and β are all positive.

sketched in Figure 1. In addition, we shall consider the question of what forces the flow through the gap.

3. The transport through the gap on a β-plane. Local and remote forcing

Our solution procedure closely follows KC. Since we assume the friction parameter $\epsilon \ll \delta$, the zero order solution can be found by integration of the inviscid version of (1) along the characteristics, i.e., lines of constant $\eta \equiv f/\delta H$. KC have shown that

$$\psi(x, \eta) = \psi(x_0, \eta) - \int_{x_0}^{x} \frac{1}{\beta} \frac{\partial \tau}{\partial y}\bigg|_{\eta} dx', \tag{6a}$$

where (x_0, y_0) is the origin at a solid boundary of the characteristic which passes through the point (x, y). As long as $dy/dx' = \delta\eta H'/\beta \neq 0$ along the characteristics (6a) can be rewritten as

$$\psi(x, y) = \psi(x_0, y_0) - \delta^{-1}\eta^{-1} \int_{y_0}^{y} \frac{\partial \tau/\partial y}{H'}\bigg|_{\eta} dy'. \tag{6b}$$

A schematic of the characteristics $\eta \equiv f/\delta H$ = constant [the coefficient $1/\delta$ is introduced to ensure that $\nabla\eta = O(1)$] is given in Figure 1. The direction of integration, shown in Figure 1 by arrows is, as in the Stommel problem, dictated by consideration of which side allows a boundary layer. The location of boundary layers is shown by bold lines. Boundary layers arise at the boundaries where the characteristics end, and inside the channel, where critical characteristics separate regions in which information comes from the different parts of the solid boundary Γ_N and Γ_S. Since we consider only the case $\delta > \delta_{cr}$ where no f/H lines close in the domain, there are a number of f/H isolines connecting Γ_N and Γ_S with the critical characteristic η_c being the westernmost. KC have shown that in the vicinity of the critical characteristics there is an internal boundary layer of width $O((\epsilon/\delta)^{1/2})$. Notice that the width of the near-wall boundary layer is substantially less: $O(\epsilon/\delta)$.

We find the transport using the auxiliary condition suggested by Kamenkovich (1961) applied at $y = y_s/2$:

$$-\int_0^1 \frac{1}{H} \frac{\partial \psi}{\partial x} dx = \int_0^1 \frac{\tau}{H} dx + \epsilon \int_0^1 \frac{1}{H^2} \frac{\partial \psi}{\partial y} dx. \tag{7}$$

Here we assumed without loss of generality that $y_s/2 < d$: it is convenient (but not essential) to apply (7) at the latitude where $f = 1$. Using (6a), (6b) in (7) and manipulating expressions yields (see Appendix)

$$2(\delta - \delta_{cr})T = 2\int_B^{1/2} \frac{\tau(y_*)}{H} dx + 2\int_A^1 \frac{\tau(y_*)}{H} dx + \left[\int_{A'}^{B} + \int_{B'}^{A}\right] \frac{\tau(x_0, y_0)}{H} dx, \tag{8}$$

where A, B are the intersections of the critical characteristics with the line $y = y_s/2$ (Fig. 1). The points A, B are defined by

$$\frac{f(y_s/2)}{H(A)} = \frac{f(0)}{H_{\min}}; \qquad \frac{f(y_s/2)}{H(B)} = \frac{f(y_s)}{H_{\max}}$$

so

$$H(A) = \frac{1-\delta}{1-\delta_{cr}}, \qquad H(B) = \frac{1+\delta}{1+\delta_{cr}};$$

$H(A') = H(A), H(B') = H(B)$ (Fig. 1). The y_*'s, the intersections of the characteristics with the lines $x = \frac{1}{2}$ and $x = 1$, respectively, are determined by

$$\frac{1}{H(x)} = \frac{1+\beta(y_* - y_s/2)}{1 \pm \delta}, \tag{9}$$

(The plus sign applies for $x = \frac{1}{2}$, the minus sign for $x = 1$.) The conditions of validity of (8) are discussed in Appendix. For the piecewise linear profile depicted in Figure 1

$$h = 1 - 4|x - 1/2| \tag{10}$$

(8) is exact.

Since the range of y_* is $(y_s/2, y_s)$ in the first integral and $(0, y_s/2)$ in the second, the transport is a weighted integral of the wind stress at all latitudes to the south of "Cape Horn" and at the "forcing regions"—loci of origins of characteristics passing through the line $y = y_s/2$ within the intervals (A', B) and (B', A). If the longitudes of the gap and the depth minimum did not exactly coincide then a band of latitudes to the north of $y = 0$ would enter in (8). This is illustrated in Figure 2. In any event the longitudes of the gap and the depth minimum cannot be too different (A should lie to the east of B') because we assume that the f/H lines do not close. The region to the south of the gap, on the other hand, enters the integration in all cases. Changing the variable of integration according to (9) and assuming little curvature we obtain

$$(\delta - \delta_{cr})T = -\frac{\beta}{H'(B)}\int_{y_s}^{y_s/2} \tau(y)\,dy - \frac{\beta}{H'(A)}\int_{0}^{y_s/2} \tau(y)\,dy + \frac{F}{2}, \tag{11}$$

where

$$F = \left[\int_{A'}^{B} + \int_{B'}^{A}\right] \frac{\tau(x_0, y_0)}{H}\,dx. \tag{12}$$

With the piecewise linear topography (10) $H'(B) = -H'(A) = 4\delta$, hence

$$T = \frac{\delta_{cr}\langle\tau\rangle/\delta + F}{2(\delta - \delta_{cr})}, \tag{13}$$

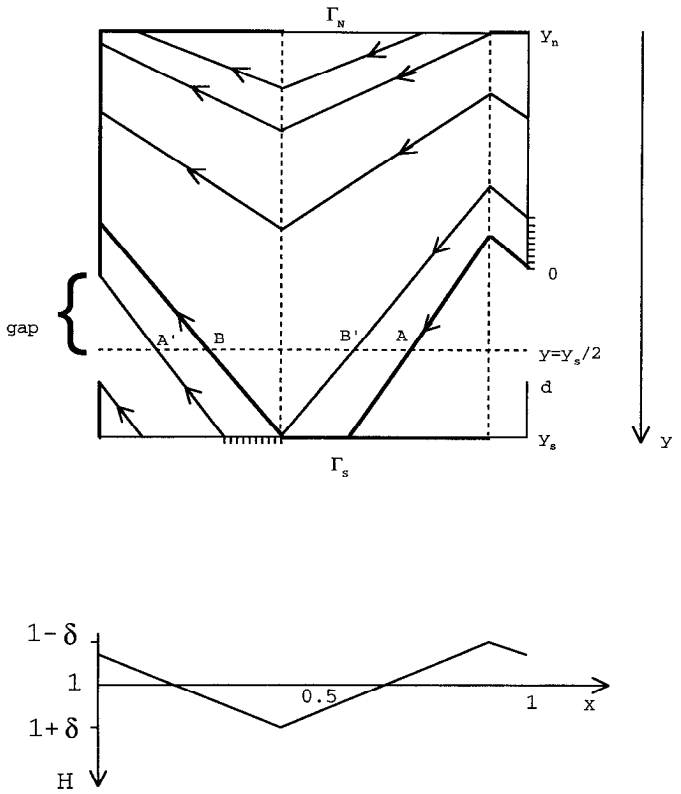

Figure 2. A variant of Figure 1: the latitudes of the gap and topographic high differ.

where

$$\langle \tau \rangle = \frac{1}{y_s} \int_0^{y_s} \tau \, dy$$

is the average wind stress to the south of "Cape Horn."

This is an asymptotic approximation to the transport in the case $\delta > \delta_{cr}$. As in KC, the transport is inversely proportional to the range of crossing isolines $R = 2(\delta - \delta_{cr})$. The novelty here is the remote forcing term F. It follows from (13) that the throughflow can be forced not only locally (i.e., by the wind at the latitudes of the gap) but also remotely by winds at the latitudes to the south of the gap and at two "forcing regions": one to the south and one to the north of the gap (shown by ticks in Fig. 1).

4. Discussion

In this paper we investigated the effects of the topographic pressure drag on the wind driven circumpolar current through the periodic gap in a rectangular basin in

the case when all lines of constant f/H are blocked by the solid boundaries. We obtained an asymptotic approximation to the transport (13) which is a generalization of the result of KC. As in KC, the transport through the gap does not depend on friction to leading order and the momentum input from wind is balanced by topographic pressure drag. If the remote forcing term F vanishes (13) reduces to the expression obtained by KC for the case of the zonal channel with vertical walls where the wind was assumed to vanish.

The important difference with KC is that the definitions of both δ_{cr} and $\langle\tau\rangle$ in (13) are based on the distance between "Cape Horn" and "Antarctica" y_s, not on the width of the gap. Inspection of Figure 1 allows one to conclude that for a given latitude of "Cape Horn" the location of remote forcing regions is independent of the width of the gap. Then it follows from (13) that the transport is independent of the width of the gap. Physically it means that topographic high is as effective in balancing the momentum input from wind as a solid boundary. The explanation to this paradoxical result is that δ_{cr} (and thus R) depends on y_s but not on the width of the gap d.

We took the gap to have zero length in our model but the results would be the same as long as the sides of the gap were not connected by f/H contours. This means that the horizontal scale of topographic variations is large compared to the length of the Drake Passage. Wang (1994) considered the opposite case where the Drake Passage had finite length and the only topographic feature is a narrow ridge fully contained inside the Drake Passage. (As is true here, it is high enough to block all the f/H contours.) His solution differs from ours in dependence of the transport on model parameters. In particular, he found the transport to depend on the coordinates of both "Cape Horn" and the poleward boundary of the gap, the latter being more important. These differences emphasize the importance of the representation of bottom topography in ocean models.

Acknowledgments. Mark Cane's numerous comments helped significantly to improve the manuscript. This work was supported by NSF grant OCE-90-00127 and by UCSIO P.O. #10058161 under Prime Agreement NA 37GP0518. This is Lamont-Doherty Earth Observatory contribution number 5330.

APPENDIX

Derivation of (8)

After integration by parts the left-hand side of (7) can be written using (6a) as

$$-\int_0^1 \frac{1}{H}\frac{\partial\psi}{\partial x}\,dx = \int_0^1 \psi(x_0, y_0)\frac{dH^{-1}}{dx}\,dx - \underbrace{\left[\int_0^B + \int_B^{1/2} + \int_{1/2}^A + \int_A^1\right]}_{I_1 \quad I_2 \quad I_3 \quad I_4}\frac{dH^{-1}}{dx}\int_{x_0}^x \frac{1}{\beta}\frac{\partial\tau}{\partial y}\bigg|_\eta dx'\,dx. \tag{A1}$$

Since $\psi(x_0, y_0) = 0$ for $B < x < A$ and $\psi(x_0, y_0) = -T$ otherwise,

$$\int_0^1 \psi(x_0, y_0) \frac{dH^{-1}}{dx} dx = -TH^{-1}\Big|_{-1+A}^{B} = \frac{2(\delta - \delta_{cr})}{1 - \delta^2} T = 2(\delta - \delta_{cr})T + O(\delta^2 T). \quad \text{(A2)}$$

For the integrals I_2, I_4 it is convenient to split the internal integrals at the extrema of H where dy/dx changes sign (Fig. 1). For example for I_2

$$\int_{x_0}^{x} \frac{1}{\beta} \frac{\partial \tau}{\partial y}\bigg|_{\eta} dx' = \int_{x_0}^{1/2} \frac{1}{\beta} \frac{\partial \tau}{\partial y}\bigg|_{\eta} dx' + \int_{1/2}^{x} \frac{1}{\beta} \frac{\partial \tau}{\partial y}\bigg|_{\eta} dx'. \quad \text{(A3)}$$

The integrals I_1, I_3 and those on the right of (A3) can be evaluated as in (6):

$$\int_{x_0}^{x} \frac{1}{\beta} \frac{\partial \tau}{\partial y}\bigg|_{\eta} dx = \delta^{-1}\eta^{-1} \int_{y_0}^{y} \frac{\partial \tau / \partial y}{H'}\bigg|_{\eta} dy = \delta^{-1}\eta^{-1}\{(H')^{-1}\}[\tau(y) - \tau(y_0)], \quad \text{(A4)}$$

where the braces denote the appropriate average. This average exists if the topography is reasonably well behaved. We further assume that

$$\{(H')^{-1}\} = \frac{1}{H'(\bar{x})}(1 + O(\delta)) \approx \frac{1}{H'(\bar{x})}, \quad \text{(A5)}$$

where $\bar{x}$ is the point where the characteristic $\eta = \eta(x)$ crosses $y = y_s/2$ (i.e. $\bar{x}$ is the point of the interval (x_0, x) such that $H(\bar{x}) = H(x)$; for I_1, I_3 and the second terms on the right of (A3) $\bar{x} = x$). Eq. (A5) will hold if either: (i) there is little change in x between y and y_0 (e.g. $\delta \gg \delta_{cr}$) or (ii) there is little curvature. For the piecewise linear profile depicted in Figure 1 the curvature is zero and this is exact.

Since $\eta^{-1}(x, y_s/2) = \delta H(x)$, using (A4), (A5) in (A1) and (A3) results in

$$\begin{aligned} -\int_0^1 \frac{1}{H} \frac{\partial \psi}{\partial x} dx \approx\ & 2(\delta - \delta_{cr})T + \int_0^1 \frac{\tau}{H} dx \\ & - \left\{ \left[\int_0^B + \int_{1/2}^A \right] \frac{\tau(x_0, y_0)}{H} dx + \left[\int_B^{1/2} + \int_A^1 \right] \frac{H'(x)}{H'(\bar{x})} \frac{\tau(x_0, y_0)}{H} dx \right\} \\ & + \int_B^{1/2} \frac{dH(x)^{-1}}{dx} H(x)\tau(y_*(1/2, x)) \left[\frac{1}{H'(x)} - \frac{1}{H'(\bar{x})} \right] dx \\ & + \int_A^1 \frac{dH(x)^{-1}}{dx} H(x)\tau(y_*(1, x)) \left[\frac{1}{H'(x)} - \frac{1}{H'(\bar{x})} \right] dx, \end{aligned} \quad \text{(A6)}$$

where the y_*'s are defined in (9). Assuming symmetry about the extrema of H implies $H'(x) = -H'(\bar{x})$. Finally, substituting (A6) in (7) yields (8).

REFERENCES

Bryan, K. and M. D. Cox. 1972. The circulation of the World ocean: a numerical study. Part I, a homogeneous model. J. Phys. Oceanogr., *2,* 319–335.

Hidaka, K. and M. Tsuchiya. 1953. On the Antarctic Circumpolar Current. J. Mar. Res., *12,* 214–222.

Johnson, J. A. and R. B. Hill. 1975. A three-dimensional model of the Southern Ocean with bottom topography. Deep-Sea Res., *22,* 745–751.

Kamenkovich, V. M. 1960. The influence of bottom relief on the Antarctic Circumpolar Current. Doklady Akademii Nauk SSSR, *134,* 983–984 (Translated from Russian).

—— 1961. The integration of the marine current theory equations in multiply connected regions. Doklady Akademii Nauk SSSR, *138,* 629–631 (Translated from Russian).

—— 1962. On the theory of the Antarctic Circumpolar Current. Trudy Instituta Okeanologii, *56,* 245–306 (Translated from Russian).

Krupitsky, A. and M. A. Cane. 1994. On topographic pressure drag in a zonal channel. J. Mar. Res., *52,* 1–22.

McWilliams, J. C., W. R. Holland and J. H. S. Chow. 1978. A description of numerical Antarctic Circumpolar Currents. Dyn. Atmos. Oceans, *2,* 213–291.

Munk, W. H. and E. Palmen. 1951. Note on the dynamics of the Antarctic Circumpolar Current. Tellus, *3,* 53–55.

Wang, L. 1994. A linear homogeneous channel model for topographic control of the Antarctic Circumpolar Current. J. Mar. Res., *52,* 649–685.

Wang, L. and R. X. Huang. 1995. Topographic control of the Antarctic Circumpolar Current. Part 1: A linear homogeneous model of wind-driven circulation in a β-plane channel. J. Phys. Oceanogr. (in press).

Wolff, J.-O. and D. J. Olbers. 1989. The dynamical balance of the Antarctic Circumpolar Current studied with an eddy resolving quasi-geostrophic model, *in* Mesoscale-Synoptic Coherent Structures in Geophysical Turbulence, J. C. J. Nihoul and B. M. Jamart, eds., Elsevier, 435–458.

Wolff, J.-O., V. O. Ivchenko, A. V. Klepikov and D. J. Olbers. 1990. On the effects of topography on the dynamics of zonal currents in the ocean. Doklady Akademii Nauk SSSR, *313,* 323–327 (Translated from Russian).

Wolff, J.-O., E. Maier-Reimer and D. J. Olbers. 1991. Wind-driven flow over topography in a zonal β-plane channel: a quasi-geostrophic model of the Antarctic Circumpolar Current. J. Phys. Oceanogr., *21,* 236–264.

Received: *19 May, 1994;* revised: *13 December, 1994.*